THE JOURNAL OF PHYSICAL CHEMISTRY B

Article

pubs.acs.org/JPCB

Cholesterol Extraction from Cell Membrane by Graphene Nanosheets: A Computational Study

Liuyang Zhang, Bingqian Xu, and Xianqiao Wang*

College of Engineering and NanoSEC, University of Georgia, Athens, Georgia 30602, United States

ABSTRACT: The health risk associated with high cholesterol levels in the human body has motivated intensive efforts to lower them by using specialized drugs. However, little research has been reported on utilizing nanomaterials to extract extra cholesterol from living tissues. Graphene possesses great potential for cholesterol extraction from cell membranes due to its distinct porous structure and outstanding surface adhesion. Here we employ dissipative dynamic simulations to explore pathways for cholesterol extraction from a cell membrane by a sheet of graphene using a coarse-grained graphene nanosheets (CGGN) model. We first demonstrate that the self-assembly process among a single layer of graphene and a group of randomly distributed cholesterol molecules in the aqueous environment, which provides a firm foundation for graphene−cholesterol interactions and the dynamic cholesterol extraction process from the cell membrane. Simulations results show that graphene is capable of removing cholesterol molecules from the bilayer membrane. The interaction between graphene and cholesterol molecules plays an important role in determining the amount of extracted cholesterol molecules from the cell membrane. Our findings open up a promising avenue to exploit the capability of graphene for biomedical applications.

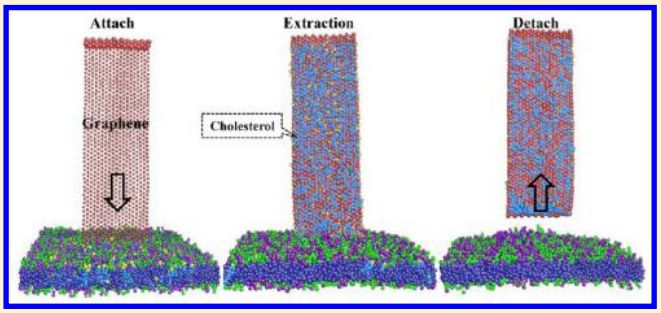

1. INTRODUCTION

Cholesterol is an abundant lipid component of mammalian cell membranes which plays an important role in maintaining the physical and mechanical properties of the membrane.[1−3] For example, it modulates the activities of membrane associated proteins, such as the function of G-protein-coupled receptor,[4] and the kinetics of current activation in voltage-gated chloride channel CIC-2.[5] It has been shown that high cholesterol level results in a decrease of membrane fluidity, and these changes are associated with a reduction in membrane permeability, a distortion of the cell contour, decreased filterability, and a shortening of the survival of cells. Therefore, there is a critical need for developing useful techniques to extract extra cholesterol from cell membranes.

Via the incorporation of cholesterol into the cellular membrane and conversion of the cholesterol into coprostanol, probiotics have enjoyed significant popularity in cholesterol extraction.[6] It has been revealed that the cyclodextrin can also cause loss of cholesterol, loss of cell viability, and altered cell morphology in bovine pulmonary artery endothelial cells.[7] Recent years have also witnessed the explosive growth of interests in investigating functionalized nanomaterials to reduce the health risks associated with high cholesterol concentration. By incorporating tryptophan and phenylalanine groups, synthesized nanosized particles with large surface areas have been utilized as suitable carriers for the adsorption of cholesterol molecules via hydrophobic interactions.[8] Hydrophobic carbon nanotubes have also been demonstrated to extract cholesterol lodgment from membrane and protein surfaces.[9] However, investigation of cholesterol extraction by two-dimensional nanomaterials such as graphene is still lacking and is worthy of exploration. Graphene, thanks to its high specific surface area and exceptional physicochemical properties,[10−15] shows great promise for cellular applications. The antibacterial materials graphene and graphene oxide nanosheets have shown the capability to induce the degradation of the inner and outer cell membrane of *Escherichia coli* and subsequently reduce the bacteria's viability. Graphene microsheets can enter cells through spontaneous membrane penetration at edge asperities and corner sites.[16] Graphyne with irregular morphology has shown intense adhesive strength to attract cholesterol molecules from the protein cluster appearing in the endothelium.[17] To demonstrate our idea of extracting cholesterol molecules from the cell membrane via graphene sheets, here we perform dissipative particle dynamics simulations to investigate its fundamental mechanisms. We will begin our study with the investigation of the self-assembly of cholesterol molecules on the surface of graphene. Then we will discuss the efficiency of cholesterol extraction from the cell membrane by tuning the binding strength between cholesterol and graphene and the evolution of interaction energy between them. Finally, we will conclude our findings with the potential impact of this proposed cholesterol extraction technique on the medical applications.

Received: October 21, 2015
Revised: January 3, 2016
Published: January 26, 2016

DOI: 10.1021/acs.jpcb.5b10330
J. Phys. Chem. B 2016, 120, 957−964

2. COMPUTATIONAL MODEL AND METHODOLOGY

Simulations are based on dissipative particle dynamics (DPD), a mesoscopic coarse-grained simulation method for soft matters and biomembrane systems.[18,19] In DPD simulation, a group of atoms is treated as a single bead located at the center of mass of the group. Beads i and j interact with each other via pairwise forces which consist of a conservative force F_{ij}^{C} representing excluded volume effect, a dissipative force F_{ij}^{D} representing viscous drag between moving beads, and a random force F_{ij}^{R} representing stochastic impulse. Both F_{ij}^{D} and F_{ij}^{R} act together as a thermostat for the beads. Similar to molecular dynamics simulation, time evolution is governed by Newton's equations of motion. The total force on bead i can be expressed as

$$F_i = \sum_{i \neq j} (F_{ij}^{C} + F_{ij}^{D} + F_{ij}^{R})$$
$$= \sum_{i \neq j} (a_{ij}\omega(r_{ij})\hat{r}_{ij} - \gamma\omega^2(r_{ij})(\hat{r}_{ij}v_{ij})\hat{r}_{ij} + \sigma\omega(r_{ij})\zeta_{ij}\Delta t^{-1/2}\hat{r}_{ij})$$

where a_{ij} is the maximum repulsive force. The entire composition of the interaction parameters is established from the literature[20−24] with empirical values summarized in Table 1.

Table 1. Soft-Repulsive Interaction Parameters a_{ij} between Lipid Molecules (L), Receptor Molecules (R), Cholesterol Molecules (C), and CGGN (G)

	L_H	L_T	R_H	R_T	C_H	C_T	G
L_H	25	100	25	100	25	100	80
L_T	100	25	100	25	100	25	80
R_H	25	100	25	100	25	100	15
R_T	100	25	100	25	100	25	80
C_H	25	100	25	100	25	100	15
C_T	100	25	100	25	100	25	a_{GC_T}
G	80	80	15	80	15	a_{GC_T}	25

The term r_{ij} represents the distance, $\hat{r}_{ij}$ the unit vector, and v_{ij} the relative velocity between beads i and j; ζ_{ij} denotes a random number with zero mean and unit variance, and

$$\omega(r_{ij}) = \begin{cases} 1 - \dfrac{r_{ij}}{r_c}, & r_{ij} < r_c \\ 0, & r_{ij} > r_c \end{cases}$$

is a normalized distribution function, r_c being the cutoff radius; γ and σ are parameters related to each other as $\sigma^2 = 2\gamma k_B T$, $k_B T$ being the unit of energy. The standard values $\sigma = 3.0$ and $\gamma = 4.5$ are used in our study.[25] The mass, length, and time scales are all normalized in the DPD simulations, with the unit of length taken to be the cutoff radius r_c, the unit of mass to be that of the solvent beads, and the unit of energy to be $k_B T$. All other quantities are expressed in terms of these basic units. The reduced DPD units can be converted to SI units by examining the membrane thickness and the lipid diffusion coefficient. The simulated value of bilayer thickness is $5r_c$, and the effective time scale of simulation can be determined from the simulated lateral diffusion constants of lipid bilayer.[26] The DPD bilayer thickness is about 4 nm with a diffusion coefficient around 5 $\mu m^2\ s^{-1}$;[27] by comparison with typical experimental values, it can be shown that one DPD length unit corresponds to approximately 0.8 nm in physical units and the time unit to τ = 24.32 ps. The time step is taken as $\Delta t = 0.01\tau$. All simulations are performed using LAMMPS.[28]

The dimension of the simulation box is $V_{box} = 40r_c \times 40r_c \times 70r_c$. The system contains a total of 327 174 particles, 302 214 water beads, and 24 960 lipid, cholesterol, and graphene beads, with a particle density of approximately 3.[29] The solvent beads are not shown for clarity. The simulation system consists of the bilayer membrane with 1600 lipid molecules (50% receptors that built into the cell membrane; receptors response to cell signals by receiving or binding to extracellular molecules), 400 cholesterol molecules, and coarse-grained graphene nanosheets (960 interconnected hydrophobic beads). As shown in Figure 1, the lipid molecule is represented by a coarse-grained model

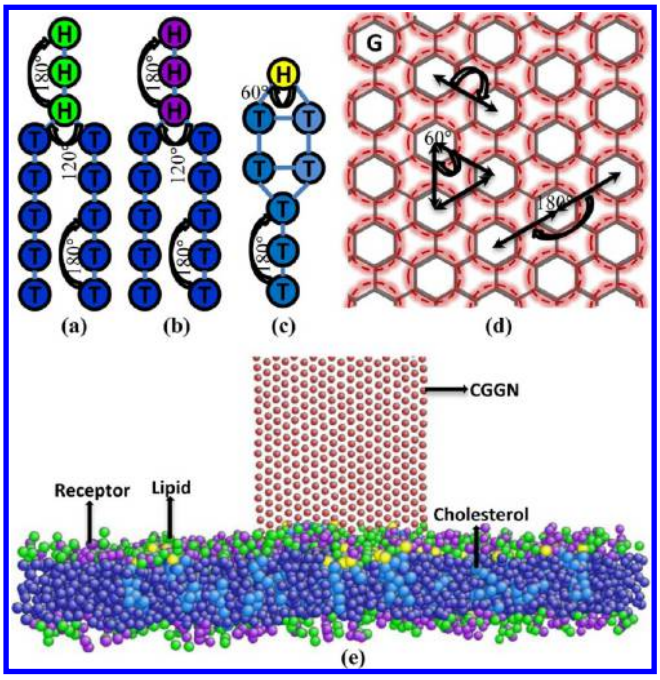

Figure 1. Schematic representation of the dissipative particle dynamics model. (a) Coarse-grained model of lipid molecule. (b) Coarse-grained model of receptor molecule. (c) Coarse-grained model of cholesterol molecule. (d) Coarse-grained graphene nanosheets (CGGN). (e) System model. In the following figures, unless otherwise stated, the lipid tails are shown in blue while the lipid heads are shown in green. The receptor tails are shown in blue while the receptor heads are shown in purple. The cholesterol tails are shown in light blue while the cholesterol heads are shown in yellow. The graphene is shown in red. For clarity, the water outside the vesicle is not shown in all figures.

with 3 hydrophilic head beads and 10 hydrophobic tail beads.[21] The cholesterol molecule is represented by a coarse-grained model with 1 hydrophilic head bead and 7 hydrophobic tail beads.[24] Coarse-grained graphene nanosheets (CGGN) is formed by grouping six carbon atoms together with bond stretch and angle bend restraints considered. During the simulation setup, all cholesterol molecules are randomly distributed in the cell membrane formed by the lipid molecules. Within a lipid molecule, cholesterol molecule, and CGGN, an elastic harmonic force

$$F_{ij}^{S} = k_s\left(1 - \frac{r_{ij}}{r_s}\right)\hat{r}_{ij}$$

is used to connect two consecutive beads, where k_s and r_s are the spring constant and equilibrium bond length, respectively.

DOI: 10.1021/acs.jpcb.5b10330
J. Phys. Chem. B 2016, 120, 957−964

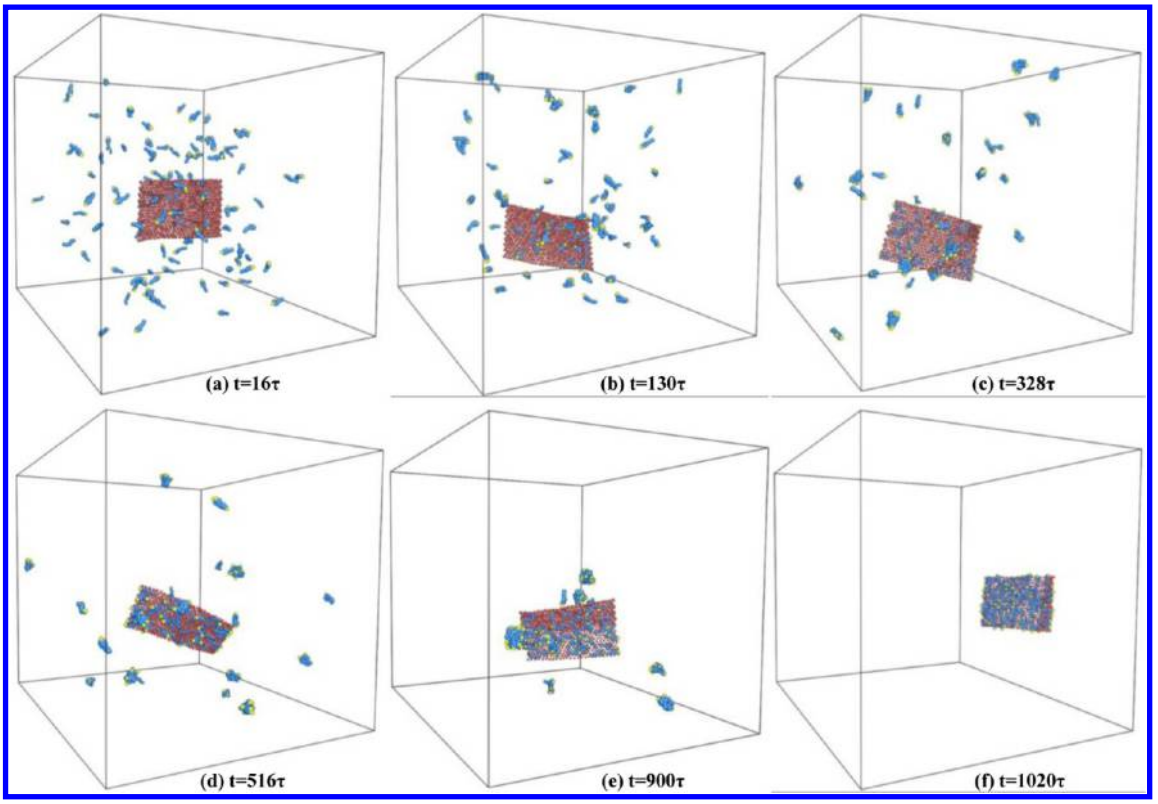

Figure 2. (a)−(f) Self-assembly of graphene sheet with cholesterol in aqueous solution from a random state.

Here we use k_s = 100.0, r_s = 0.7r_c for lipid and cholesterol molecule[24,30] and k_s = 10.0, r_s = 0.1 for CGGN beads.[23] The bending resistance of the lipid molecule, cholesterol molecule, and CGGN is represented as an additional force due to a harmonic constraint on two consecutive bonds

$$F^{\theta} = -\nabla V_{\text{bend}} = -\nabla[k_{\theta}(\theta - \theta_0)^2]$$

where k_θ, θ, and θ_0 are the bending constant, inclination angle, and equilibrium angle, respectively. For the lipid molecule, three consecutive lipid tail beads or three consecutive lipid head beads in a lipid molecule, we take k_θ = 6 and θ_0 = 180°; for the last head bead and the top tail beads k_θ = 3 and θ = 120°; for the bottom two consecutive head beads and the first bead in each tail k_θ = 4.5 and θ = 120°.[25] For the cholesterol molecule, the bond between the head bead and the first two tail beads and the bond between the first four tail beads and the last tail beads, we take k_θ = 100 and θ = 60°. For the first four tail beads, we take k_θ = 3 and θ = 90°. For the consecutive tail beads, we take k_θ = 6 and θ = 180°.[24] In order to maintain the honeycomb structure and two-dimensional properties of graphene, harmonic bend potentials for 60° and 180° angles are applied on the equilateral triangle geometry and the linear structure with 3 neighboring beads, respectively. The bending constant for CGGN is chosen as k_θ = 30. It has been revealed that the equilibrium CGGN exhibits a rectangular shape with uniform bond length and flat surface properties when the bending constants were above 30k_BT per rad^2.[23]

3. RESULTS AND DISCUSSION

3.1. Self-Assembly. Cholesterol is recognized as a useful building block, which upon incorporation into polymer provides remarkable influence on self-assembly in the aqueous solution. The hydrophobic nature and strong self-associative interaction of cholesterol are postulated to provide the driving force for self-assembling into nanostructures. Because of hydrophobicity, it is expected to understand the intermolecular interaction between graphene and cholesterol molecules. A rectangular CGGN with a size of 25r_c × 16r_c is introduced in the simulation box of $V_{\text{box}} = (60r_c)^3$, with 144 cholesterol molecules. Figure 2 shows the time evolution of the self-assembly of graphene sheet and cholesterol molecules. At the beginning of simulation, the cholesterol molecules are randomly dispersed in the water beads and are adjusted to prevent errant penetration into the graphene sheet. The cholesterol molecules immediately start to agglomerate and adsorb onto the graphene sheet surface due to the hydrophobicity of the cholesterol tail. As time goes on, graphene sheet/cholesterol hybrid structures are accompanied by spherical clusters purely formed by cholesterol molecules in the simulation box. It is observed that the cluster collapses and adheres to the surface of graphene sheet when it draws close enough to the graphene sheet. To further clarify the adsorption of cholesterol molecules, the time evolution of adsorption is calculated by the radius of gyration R_g of all cholesterol molecules[31]

$$R_g = \sqrt[2]{\frac{1}{n}\sum |r_i^2 - r_{\text{com}}^2|} \quad (1)$$

where n is the number of cholesterol molecules, r_i is the position of the center of mass of the ith cholesterol molecule, and r_{com} is the position of the center of mass of all cholesterol molecules. In Figure 3, by setting the interaction between the G beads and the T beads in the cholesterol molecule as a_{GCT} = 15, R_g shows a linear decreasing function in which the slope is negative, indicating that the cholesterol molecules aggregate and attach onto the graphene sheet. R_g with a large value

DOI: 10.1021/acs.jpcb.5b10330
J. Phys. Chem. B 2016, 120, 957−964

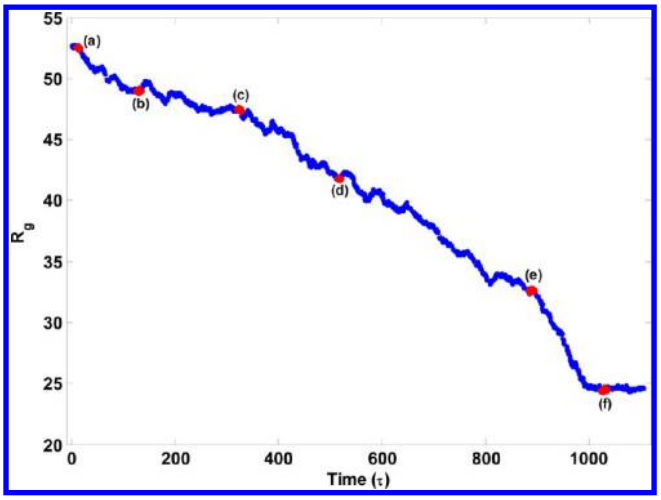

Figure 3. Radius of gyration of cholesterol molecules in the aqueous solution. (a)−(f) correspond to the snapshot in Figure 2.

indicates that the cholesterol molecules have a random and sparse distribution in the system. After R_g reaches the minimum value of 24.6, almost all the cholesterol molecules are absorbed by the graphene sheet and form a stable structure. Simulation results related to self-assembly process of the graphene and cholesterol molecules suggest that the graphene can adsorb cholesterol molecules by the hydrophobic interaction between the graphene benzene rings (G beads) and cholesterol hydrocarbons (T beads).

3.2. Effect of Entry Orientation. Since we intend to utilize graphene to extract cholesterols from the cell membrane, how to install the graphene on the cell membrane becomes crucial in order to achieve maximum extraction efficiency with minimum disruption to the cell membrane. Graphene docking on the cell membrane is positioned into two different orientations, horizontal and perpendicular to the cell membrane, depending on the preference on the binding site between the graphene sheet and cell membrane receptors. In simulations, to enhance the probability of graphene sheet interacting with the bilayer and to reduce the waiting time, we place the graphene sheet

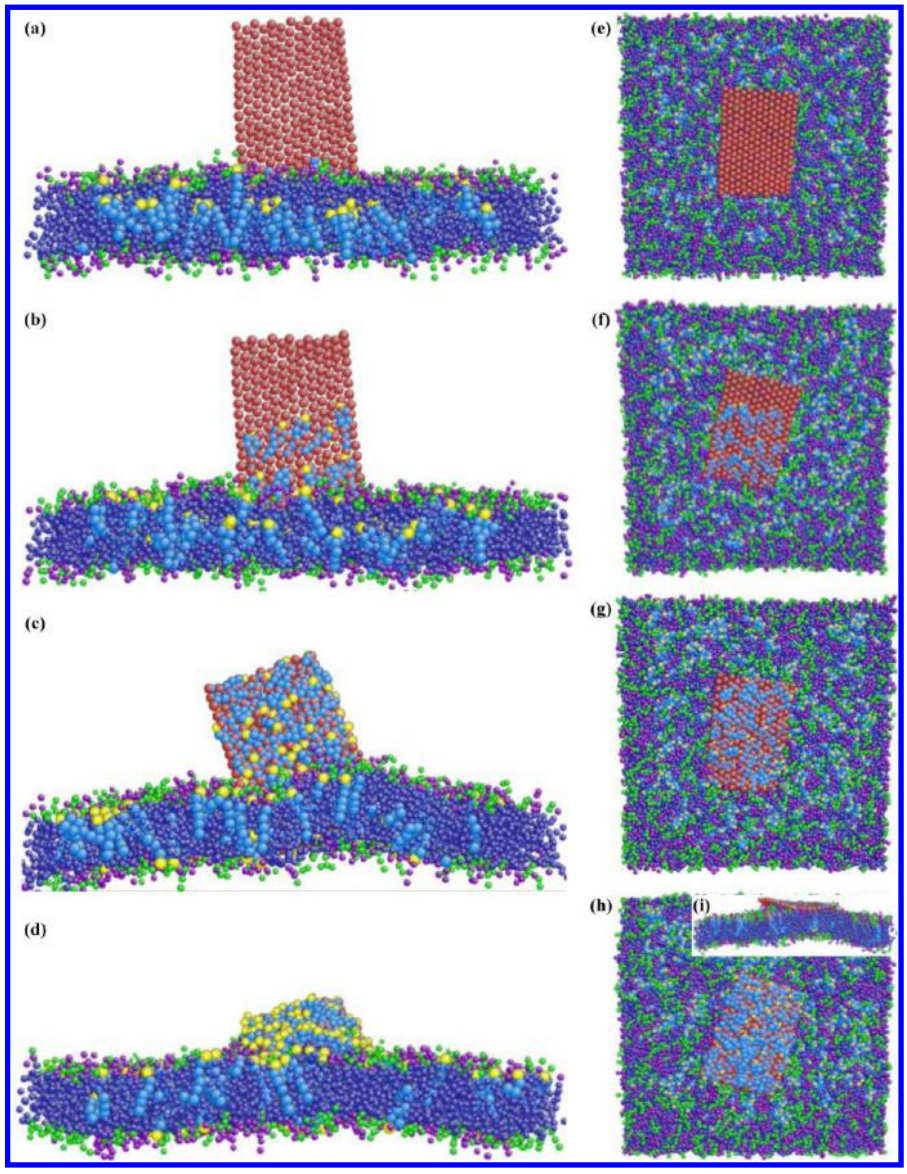

Figure 4. Orientation of graphene sheet (a)−(d) vertical orientation; (e)−(h) horizontal orientation; (i) cross-section view of horizontal orientation.

DOI: 10.1021/acs.jpcb.5b10330
J. Phys. Chem. B 2016, 120, 957−964

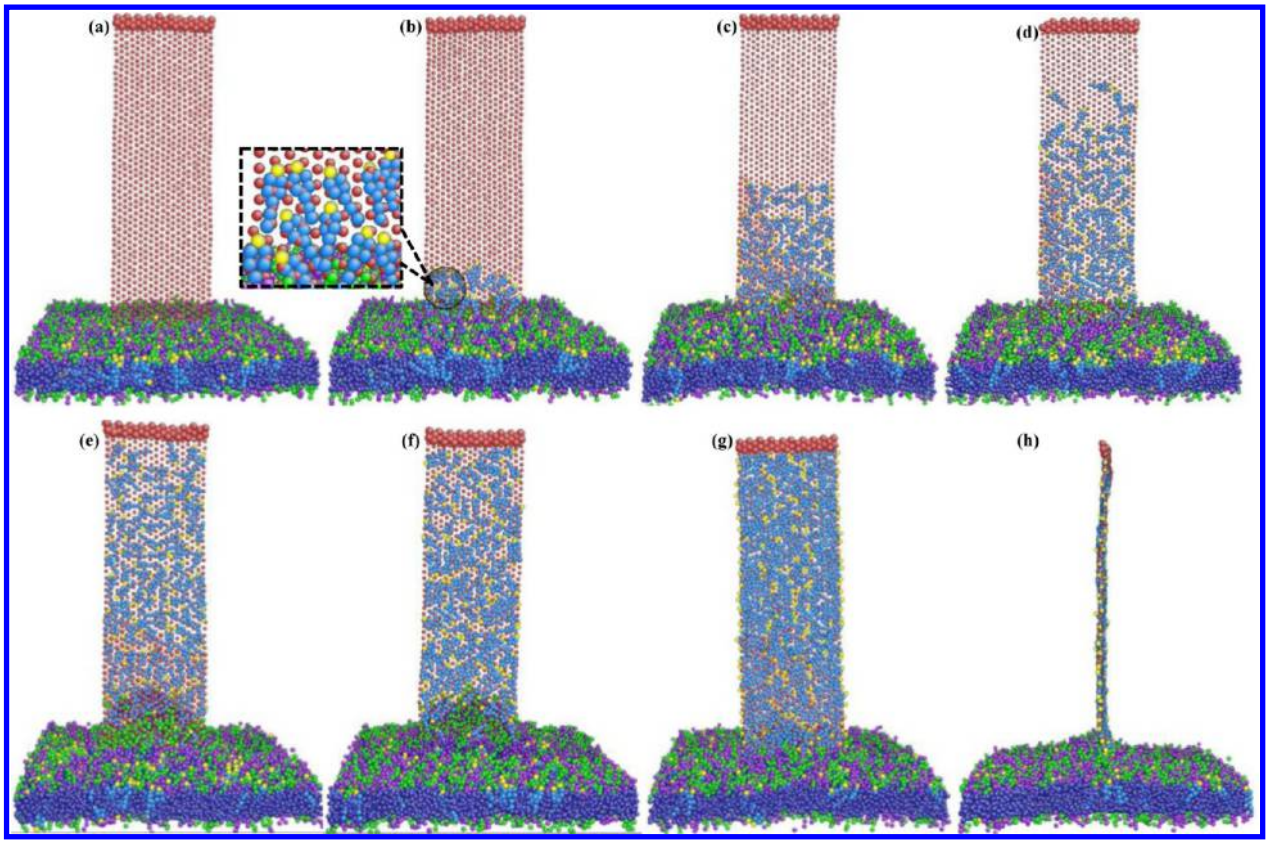

Figure 5. Representative trajectories of extraction of cholesterol from cell membrane.

close to the membrane within a perpendicular distance of r_c for all simulated orientation. As shown in Figure 4a–d, the free graphene sheet is put vertically above the membrane. Experiments and simulations both show that graphene microsheets primarily enter cells through spontaneous membrane penetration at edge asperities and corner sites.[16,32] Cholesterol molecules can spontaneously adsorb to the graphene sheet surface and are extracted from the membrane as long as the interaction between graphene sheet and cholesterol molecules is stronger than that between cholesterol molecules and lipids. Accompanying the accumulation of cholesterol molecules on the surface of the graphene sheet, the graphene sheet slightly tilts and slowly penetrates into the cell membrane due to the strong interaction between the cholesterol molecules on the graphene sheet and the bilayer hydrophobic core. However, the hydrophilic portion of cholesterol molecules prevents the graphene sheet covered with cholesterol molecules from being internalized by the hydrophobic core of the membrane bilayer. Finally, the graphene sheet lays down on the surface of the membrane. On the contrary, when the graphene sheet is docked in parallel with the cell membrane as shown in Figure 4e–h, the cholesterol molecules gathers toward the area covered by the graphene sheet. The horizontal placement of graphene increases the contact area between the graphene sheet and the cell membrane which make it easy to absorb the cholesterol molecules from the cell membrane. In this case, the graphene sheet keeps its initial orientation and cannot enter the bilayer either. The cross-section view of the horizontal placement of graphene shown in Figure 4i indicates that the graphene stays on the surface of cell membrane and is not able to penetrate into the cell membrane. The parallel docked graphene sheet does not perfectly act to extract the cholesterol molecules from the cell membrane. Instead, it increases the cholesterol concentration in the area around the graphene sheet. The transition of the graphene sheet orientation is in a good agreement with the phenomenon seen in graphene nanosheets into cell membranes from other researchers' work.[32] The docking orientation of the graphene sheet determines the extraction efficiency of cholesterol molecules from the cell membrane.

3.3. Quantitative Data on Cholesterol Extraction. *Centre of Mass.* With the aim of extracting cholesterol molecules from the cell membrane, the vertically docked graphene sheet possesses a high potential as an independent carrier to extract cholesterol from the cell membrane when compared with the parallel docked graphene sheet. However, it has been demonstrated that the direct contact with extremely sharp edges of the graphene sheet can penetrate and cut bacterial cell membranes.[33] Therefore, a free vertically docked graphene sheet is not suitable to extract the cholesterol efficiently unless the position of graphene sheet is constrained; otherwise, it may damage the cell membrane. One way to model this in computer simulations is to restrict the motion of a portion of the G beads on the edge of graphene sheet away from the cell. The initial suspended distance from the membrane surface is dependent on the angle bending coefficient. The angle bending coefficient $30k_BT$ keeps the graphene sheet stretched in the plane; therefore, the initial suspending distance from the cell membrane is within the range $0.5-2r_c$. Our unbiased simulations in Figure 5 clearly show that the suspended graphene sheet can extract cholesterol molecules from the cell membrane. Two distinguishable modes are observed: (i) attaching mode and (ii) extraction mode. In the

DOI: 10.1021/acs.jpcb.5b10330
J. Phys. Chem. B 2016, 120, 957–964

attaching mode, the graphene sheet with its initially unbiased orientation undergoes a swing motion, back and forth, around the fixed edge. The other end of the graphene sheet eventually attaches to the cell membrane due to the strong interaction between cell membrane receptors and the graphene sheet. This downward end of graphene is allowed to swing around the surface of cell membrane during the entire simulation, and the graphene sheet is incapable to penetrate into the cell membrane due to the predefined confinement. In the extraction mode, the randomly distributed cholesterol molecules start to vigorously climb up to the graphene sheet surface. The density of cholesterol molecules on the graphene sheet increases as cholesterol molecules are extracted from the cell membrane and climb up the graphene sheet. Our simulation also shows that when the whole graphene sheet with extracted cholesterol molecules in Figure 5g is pulled up, it detaches the cell membrane without deteriorating the cell membrane structure. The diffusivity of water perpendicular to the cell membrane provides a useful way to test the porosity of the bilayers after extraction process is finished. We solve the diffusion equation for the mean-square displacement of water molecules in the z-direction. A least-squares fit is used to fit the MSD to a straight line, and the Einstein relation can then be used to calculate the diffusion coefficient $D = (1/2nt)\langle(r_i(t) - r_i(0))^2\rangle$, where n is the number of dimensions, t is time, and r_i is the position of water molecule i. The water diffusion coefficient perpendicular to the graphene sheet keeps almost unchanged with the value of $0.0141r_c^2/\tau$ before and after the extraction process, indicating that there is no significant water penetration into the cell membrane and during the simulation the membrane keeps its integrity.

To better understand the whole extraction process, we analyze the movement of the center of mass (CoM) of cholesterol molecules on the surface of graphene sheet. Figure 6 shows the time evolution of the CoM of cholesterol

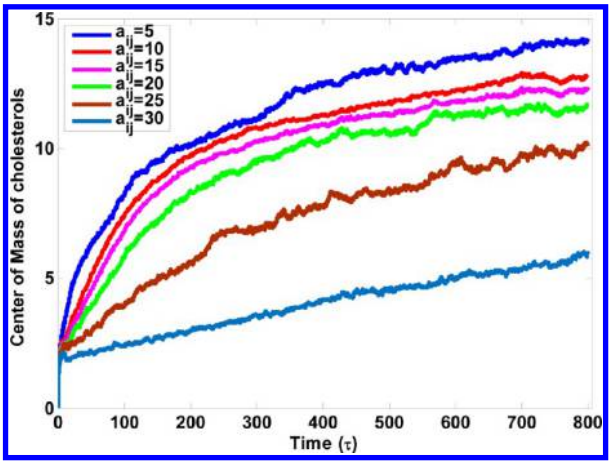

Figure 6. Time evolution of the CoM of cholesterol along the z-direction toward the graphene sheet for the representative trajectories shown in Figure 5.

molecules with a simulation model shown in Figure 5. The initial nonzero CoM represents the instant attaching mode between the graphene sheet and cell membrane. During the extraction mode, the gradual increase in the CoM corresponds to the substantial extraction of cholesterol molecules from the membrane. As the number of cholesterol molecules in the membrane decreases and the restraining effect from the exposure of their hydrophobic tails to water evolves, the subsequent increase of the CoM slows down. The strong attraction between the graphene sheet and cholesterol molecules largely depends on the graphene sheet's unique 2D structure which facilitates exceptionally strong dispersion interactions between the graphene sheet and small molecules.[17,34] Another way to show the robustness of cholesterol extraction by graphene sheet is to artificially adjust the repulsive force a_{ij} between graphene sheet and cholesterol molecules tail. Following the same procedure, the extraction process under different a_{GCT} is used. When a relatively low a_{GCT} is used, the interaction between the graphene sheet and cholesterol molecules remains strong between cholesterol molecules and lipid molecules. Therefore, a large portion of cholesterol molecules can be continuously extracted from the membrane. It should be noticed that the maximum repulsive force between lipid tail and cholesterol tail can be set to be $a_{GCT} = 25$. Thus, for a relatively high a_{GCT} close to this value, the cholesterol molecules prefer to stay inside the cell membrane and fewer cholesterol molecules can be extracted from the membrane. Quantitatively speaking, the graphene sheet can extract cholesterol molecules efficiently from the cell membrane when a_{GCT} is less than 25 between graphene sheet and cholesterol molecules.

Interaction Energy. The physical interaction between the graphene sheet and cholesterol molecules is also analyzed during the whole extraction process. Figure 7 depicts the time

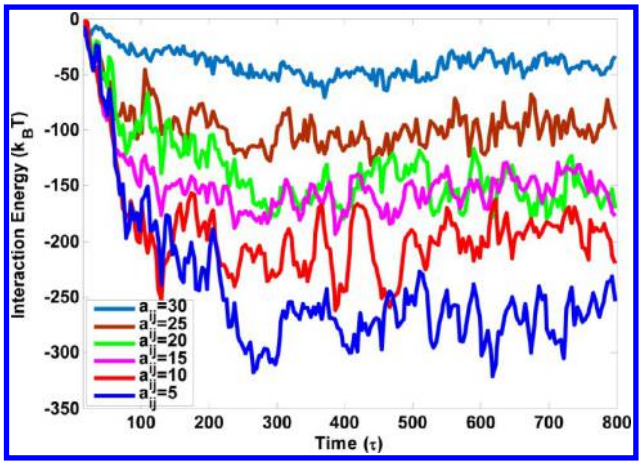

Figure 7. Time evolution of the interaction energy between the graphene sheet and cholesterol molecules for the representative trajectories shown in Figure 5.

evolution of the interaction energy profile between the graphene sheet and cholesterol molecules during the extraction process. By varying the interaction a_{GCT} between the graphene sheet and cholesterol molecules from high to low values, the initial energy drop describes a quick absorption of cholesterol molecules on the graphene surface after the attaching mode. The low-energy plateau corresponds to a slow accumulation of cholesterol molecule on the graphene sheet surface. The negative sign of the interaction energy indicates that the state where the cholesterol molecules are absorbed on the graphene sheet surface is preferable by comparison of the state where cholesterol molecules are randomly distributed in the membrane. Once the cholesterol molecules attach to the graphene sheet, a complex and collective movement of cholesterol molecules toward the graphene sheet surface is

DOI: 10.1021/acs.jpcb.5b10330
J. Phys. Chem. B 2016, 120, 957−964

attributed to the hydrophobic interactions between graphene sheet and cholesterol tails. The energy profile can further support the evolution of the CoM of cholesterol molecules in Figure 6. Because of the exceptionally large flat surface of the graphene sheet, the graphene sheet possesses in principle a robust capability for extracting cholesterol molecules from the cell membrane.

Cell Membrane Deformation. It should be noticed that graphene can induce cytotoxicity to red blood cells.[35] The cholesterol extraction capability of the graphene sheet could also introduce disturbance to the cell membrane. Many cell processes ranging from vesicle trafficking to actin assembly involve shape changes and are thus affected by the intrinsic deformability of the cell membrane.[36] The disruptive extraction of cholesterol molecules leads not only to a sparser lipid bilayer but also to a deformation of the membrane due to strong dragging forces from the graphene sheet, thus resulting in the loss of cell membrane integrity. We characterize the membrane integrity by calculating the local membrane curvature in the final extraction state based on the method developed by Yue et al.[37] The membrane surface is divided into $2r_c \times 2r_c$ vertical square prisms unit, and the lipids within each unit determine the center of mass of that unit. The geometric surface representing the membrane via least-squares fitting is described in the form of quantic polynomial, $z(x,y) = \sum_{i+j\leq 5} a_{ij} x^i y^j$, where a_{ij} are fitted parameters, and the curvature k_x and k_y at point (x, y) can be evaluated via

$$k_x = \frac{\mathrm{d}^2 z}{\mathrm{d}x^2} \Bigg/ \left[1 + \left(\frac{\mathrm{d}z}{\mathrm{d}x}\right)^2\right]^{3/2}, \quad k_y = \frac{\mathrm{d}^2 z}{\mathrm{d}x^2} \Bigg/ \left[1 + \left(\frac{\mathrm{d}z}{\mathrm{d}y}\right)^2\right]^{3/2} \tag{5}$$

It can be noticed, from Figure 8, that the membrane curvature decreases as the interaction between the graphene sheet and cholesterol molecules increases, which indicates the enhanced extraction of cholesterol molecules by the graphene sheet could cause the damage on the membrane. Our results can further verify the fact that the cholesterol molecules have the potential to generate a large membrane curvature[38] and affect the mechanical properties of the cell membrane.[1,3]

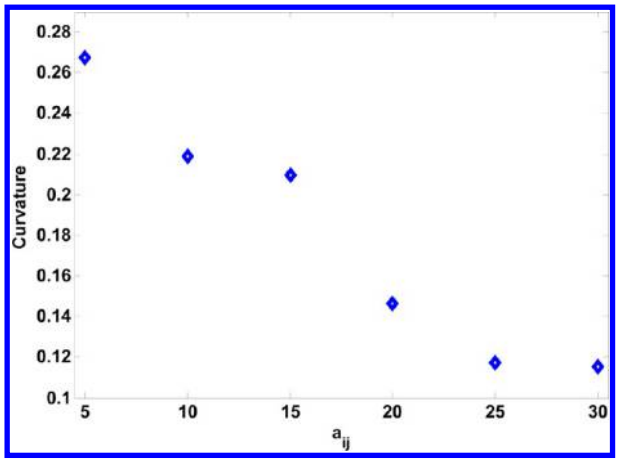

Figure 8. Maximal curvature of the planar membrane for various a_{ij}.

4. CONCLUDING REMARKS

In summary, we have performed dissipative particle dynamics simulations to investigate how the graphene sheet extracts the cholesterol molecules from a cell membrane. Through investigating the self-assembly process of the cholesterol molecules and the graphene sheet, we find that the graphene sheet has the capability to absorb the cholesterol molecules on its surface. Our simulation also presents the optimal docking orientation of a graphene sheet on cell membrane for the maximum extraction efficiency. The vertical docking orientation with a fixed end is chosen as it can truly demonstrate the extraction process and does not damage the cell membrane structure. The cooperative movements of extracted cholesterol molecules are also observed on the two-dimensional graphene sheet surface due to the redistribution of hydrophobic tails to maximize hydrophobic interaction with graphene sheet surface. The extraction of cholesterol molecules from the cell membrane can induce serious membrane curvature disruption and thus probably reduce cell viability. Our findings allow the assessment of graphene implication in reducing the health risk associated with high cholesterol level.

AUTHOR INFORMATION

Corresponding Author

*Tel 706-5426251; e-mail xqwang@uga.edu (X.W.).

Notes

The authors declare no competing financial interest.

ACKNOWLEDGMENTS

The authors acknowledge support from the National Science Foundation (Grant CMMI-1306065) and University of Georgia (UGA) start-up fund. The facility support for modeling and simulations from the UGA Advanced Computing Resource Center is greatly appreciated.

REFERENCES

(1) Hissa, B.; Pontes, B.; Roma, P. M.; Alves, A. P.; Rocha, C. D.; Valverde, T. M.; Aguiar, P. H.; Almeida, F. P.; Guimaraes, A. J.; Guatimosim, C.; et al. Membrane Cholesterol Removal Changes Mechanical Properties of Cells and Induces Secretion of a Specific Pool of Lysosomes. *PLoS One* **2013**, *8*, e82988.

(2) Khelashvili, G.; Harries, D. How Cholesterol Tilt Modulates the Mechanical Properties of Saturated and Unsaturated Lipid Membranes. *J. Phys. Chem. B* **2013**, *117*, 2411−2421.

(3) Khatibzadeh, N.; Gupta, S.; Farrell, B.; Brownell, W. E.; Anvari, B. Effects of Cholesterol on Nano-Mechanical Properties of the Living Cell Plasma Membrane. *Soft Matter* **2012**, *8*, 8350−8360.

(4) Pucadyil, T. J.; Chattopadhyay, A. Role of Cholesterol in the Function and Organization of G-protein Coupled Receptors. *Prog. Lipid Res.* **2006**, *45*, 295−333.

(5) Hinzpeter, A.; Fritsch, J.; Borot, F.; Trudel, S.; Vieu, D.-L.; Brouillard, F.; Baudouin-Legros, M.; Clain, J.; Edelman, A.; Ollero, M. Membrane Cholesterol Content Modulates ClC-2 Gating and Sensitivity to Oxidative Stress. *J. Biol. Chem.* **2007**, *282*, 2423−2432.

(6) Lye, H. S.; Rusul, G.; Liong, M. T. Removal of Cholesterol by Lactobacilli via Incorporation and Conversion to Coprostanol. *J. Dairy Sci.* **2010**, *93*, 1383−1392.

(7) Kline, M.; O'Connor Butler, E. S.; Hinzey, A.; Sliman, S.; Kotha, S.; Marsh, C.; Uppu, R.; Parinandi, N. A Simple Method for Effective and Safe Removal of Membrane Cholesterol from Lipid Rafts in Vascular Endothelial Cells: Implications in Oxidant-Mediated Lipid Signaling. In *Free Radicals and Antioxidant Protocols*; Uppu, R. M., Murthy, S. N., Pryor, W. A., Parinandi, N. L., Eds.; Humana Press: 2010; Vol. *610*, pp 201−211.

(8) Kalburcu, T.; Ozturk, N.; Tuzmen, N.; Akgol, S.; Denizli, A. Cholesterol Removal onto the Different Hydrophobic Nanospheres: A Comparison Study. *J. Ind. Eng. Chem.* **2014**, *20*, 153−159.

DOI: 10.1021/acs.jpcb.5b10330
J. Phys. Chem. B 2016, 120, 957−964

(9) Gburski, Z.; Gorny, K.; Raczynski, P. The Impact of a Carbon Nanotube on the Cholesterol Domain Localized on a Protein Surface. *Solid State Commun.* **2010**, *150*, 415−418.
(10) Zhang, L.; Wang, X. Atomistic Insights into the Nanohelix of Hydrogenated Graphene: Formation, Characterization and Application. *Phys. Chem. Chem. Phys.* **2014**, *16*, 2981−2988.
(11) Zhang, L.; Wang, X. Computational Insights of Water Droplet Transport on Graphene Sheet with Chemical Density. *J. Appl. Phys.* **2014**, *115*, 194306.
(12) Zhang, L.; Becton, M.; Wang, X. Mechanical Analysis of Graphene-Based Woven Nano-Fabric. *Mater. Sci. Eng., A* **2015**, *620*, 367−374.
(13) Becton, M.; Zhang, L.; Wang, X. On the Crumpling of Polycrystalline Graphene by Molecular Dynamics Simulation. *Phys. Chem. Chem. Phys.* **2015**, *17*, 6297−6304.
(14) Zhang, L.; Zeng, X.; Wang, X. Programmable Hydrogenation of Graphene for Novel Nanocages. *Sci. Rep.* **2013**, *3*, 3162.
(15) Becton, M.; Zhang, L.; Wang, X. Effects of Surface Dopants on Graphene Folding by Molecular Simulations. *Chem. Phys. Lett.* **2013**, *584*, 135−141.
(16) Li, Y.; Yuan, H.; von dem Bussche, A.; Creighton, M.; Hurt, R. H.; Kane, A. B.; Gao, H. Graphene Microsheets Enter Cells through Spontaneous Membrane Penetration at Edge Asperities and Corner Sites. *Proc. Natl. Acad. Sci. U. S. A.* **2013**, *110*, 12295−12300.
(17) Zhang, L.; Wang, X. Mechanisms of Graphyne-Enabled Cholesterol Extraction from Protein Clusters. *RSC Adv.* **2015**, *5*, 11776−11785.
(18) Groot, R. D.; Rabone, K. L. Mesoscopic Simulation of Cell Membrane Damage, Morphology Change and Rupture by Nonionic Surfactants. *Biophys. J.* **2001**, *81*, 725−736.
(19) Groot, R. D.; Warren, P. B. Dissipative Particle Dynamics: Bridging the Gap between Atomistic and Mesoscopic Simulation. *J. Chem. Phys.* **1997**, *107*, 4423−4435.
(20) Zhang, L.; Wang, X. Nanotube-Enabled Vesicle−Vesicle Communication: A Computational Model. *J. Phys. Chem. Lett.* **2015**, *6*, 2530−2537.
(21) Zhang, L.; Becton, M.; Wang, X. Designing Nanoparticle Translocation through Cell Membranes by Varying Amphiphilic Polymer Coatings. *J. Phys. Chem. B* **2015**, *119*, 3786−3794.
(22) Zhang, L.; Wang, X. Coarse-Grained Modeling of Vesicle Responses to Active Rotational Nanoparticles. *Nanoscale* **2015**, *7*, 13458−13467.
(23) Min, S. H.; Lee, C.; Jang, J. Dissipative Particle Dynamics Modeling of a Graphene Nanosheet and Its Self-assembly with Surfactant Molecules. *Soft Matter* **2012**, *8*, 8735−8742.
(24) de Meyer, F. J.; Rodgers, J. M.; Willems, T. F.; Smit, B. Molecular Simulation of the Effect of Cholesterol on Lipid-Mediated Protein-Protein Interactions. *Biophys. J.* **2010**, *99*, 3629−3638.
(25) Li, Y.; Li, X.; Li, Z.; Gao, H. Surface-Structure-Regulated Penetration of Nanoparticles Across a Cell Membrane. *Nanoscale* **2012**, *4*, 3768−3775.
(26) Li, X.; Liu, Y.; Wang, L.; Deng, M.; Liang, H. Fusion and Fission Pathways of Vesicles from Amphiphilic Triblock Copolymers: A Dissipative Particle Dynamics Simulation Study. *Phys. Chem. Chem. Phys.* **2009**, *11*, 4051−4059.
(27) Shillcock, J. C.; Lipowsky, R. Tension-Induced Fusion of Bilayer Membranes and Vesicles. *Nat. Mater.* **2005**, *4*, 225−228.
(28) Plimpton, S. Fast Parallel Algorithms for Short-Range Molecular Dynamics. *J. Comput. Phys.* **1995**, *117*, 1−19.
(29) Nielsen, S. O.; Ensing, B.; Ortiz, V.; Moore, P. B.; Klein, M. L. Lipid Bilayer Perturbations around a Transmembrane Nanotube: A Coarse Grain Molecular Dynamics Study. *Biophys. J.* **2005**, *88*, 3822−3828.
(30) Venturoli, M.; Smit, B.; Sperotto, M. M. Simulation Studies of Protein-Induced Bilayer Deformations, and Lipid-Induced Protein Tilting, on a Mesoscopic Model for Lipid Bilayers with Embedded Proteins. *Biophys. J.* **2005**, *88*, 1778−1798.
(31) Becton, M.; Zhang, L.; Wang, X. Mechanics of Graphyne Crumpling. *Phys. Chem. Chem. Phys.* **2014**, *16*, 18233−18240.
(32) Wang, J.; Wei, Y.; Shi, X.; Gao, H. Cellular Entry of Graphene Nanosheets: the Role of Thickness, Oxidation and Surface Adsorption. *RSC Adv.* **2013**, *3*, 15776−15782.
(33) Akhavan, O.; Ghaderi, E. Toxicity of Graphene and Graphene Oxide Nanowalls against Bacteria. *ACS Nano* **2010**, *4*, 5731−5736.
(34) Lazar, P.; Karlický, F.; Jurečka, P.; Kocman, M.; Otyepková, E.; Šafářová, K.; Otyepka, M. Adsorption of Small Organic Molecules on Graphene. *J. Am. Chem. Soc.* **2013**, *135*, 6372−6377.
(35) Liao, K.-H.; Lin, Y.-S.; Macosko, C. W.; Haynes, C. L. Cytotoxicity of Graphene Oxide and Graphene in Human Erythrocytes and Skin Fibroblasts. *ACS Appl. Mater. Interfaces* **2011**, *3*, 2607−2615.
(36) Diz-Muñoz, A.; Fletcher, D. A.; Weiner, O. D. Use the Force: Membrane Tension as an Organizer of Cell Shape and Motility. *Trends Cell Biol.* **2013**, *23*, 47−53.
(37) Yue, T.; Li, S.; Zhang, X.; Wang, W. The Relationship between Membrane Curvature Generation and Clustering of Anchored Proteins: A Computer Simulation Study. *Soft Matter* **2010**, *6*, 6109−6118.
(38) Zimmerberg, J.; Kozlov, M. M. How Proteins Produce Cellular Membrane Curvature. *Nat. Rev. Mol. Cell Biol.* **2006**, *7*, 9−19.

DOI: 10.1021/acs.jpcb.5b10330
J. Phys. Chem. B 2016, 120, 957−964